

OPTICAL SIMULATION TO ENHANCE PV MODULE ENCAPSULATION

S. Krauter^{1,2} and P. Grunow²

Technical University Berlin, Sec. EM4, Einsteinufer 11, 10587 Berlin, Germany

Tel: +49-30-314-22403, Fax: +49-30-314-21133

Photovoltaic Institute Berlin, c/o Einsteinufer 25, 10587 Berlin, Germany

Tel: +49-30-314-25977, Fax: +40-30-314-26617

e-mail: krauter@pi-berlin.com, grunow@pi-berlin.com

ABSTRACT: This paper presents a simulation tool to examine the optical transmission of any encapsulation of PV modules under real-world conditions in order to compare various types of encapsulation materials and front covers, with and without anti-reflective-coatings. While standard test conditions are using a fixed spectrum at perpendicular incidence only, real world performance is more complex with various spectra, incidence angles and presence of polarization. The model developed is consequently linked with a precise simulation of the actual irradiance condition at each moment of a clear day also considering dispersion (change of refractive indices with the optical wavelength) and multiple internal reflections inside and among the layers. To calculate and compare life-cycle yields, numerous instants (each 15 minutes) of actual transmittance, actual irradiance, efficiency and electrical power output are added-up to a daily and yearly energy yield. The model is an appropriate tool to optimize the optical layout of the encapsulation, including the use of new encapsulation materials (e.g., TPU instead of EVA) and additional anti-reflective-layers on the cover glass, considering not standard test conditions only, but real world applications at different locations (e.g., Central Europe, Southern Europe, Tropics, etc.).

Keywords: optical losses, encapsulation, ray tracing.

1 INTRODUCTION

Typically solar cells are developed to show best performance under laboratory conditions for a standard AM 1.5 spectrum, perpendicular irradiance at level of 1,000 W/m² and room temperature (25°C). Performance measurements are usually carried out using a solar cell to air interface.

These conditions do not reflect the real world. Solar cells are regularly encapsulated within two additional optical slabs, typically EVA and glass, irradiance is hardly ever perpendicular, spectrum is rarely AM 1.5, and operation temperature for relevant irradiance levels is well above room temperature (15–30 K higher) for non-alpine or non-arctic applications. Irradiance level infrequently reaches 1,000 W/m², even for locations with good conditions. This situation leads to considerable uncertainties for the accumulated electrical energy yield of PV modules. Therefore a simulation toolbox was created to increase yield accuracy considering optical, thermal and electrical parameters (see Fig. 1). This publication is focusing on the optical parameters and the optical simulation of that issue. Two stages are considered: the cell-module interface and module to real world interface, also considering actual spectra, irradiance levels, incidence angles and polarization.

1.1 Cell to module interface

The module manufacturer usually acquires solar cells probed and optimized using an optical interface consisting of the solar cell and the surrounding air. Usually the integration of the cell into a module encapsulation boosts the electrical power output by 1–2% due to the better matching of the optical interfaces involved: Antireflection coating ($n_{AR} = 1.9–2.3$) to EVA ($n_{EVA} = 1.45$) to glass ($n_{Glass} = 1.54$) to air ($n_{Air} = 1.0$) instead of antireflection coating to air only. Therefore accumulated reflection losses are reduced, the photon flux is increased, so is the photo current and power output.

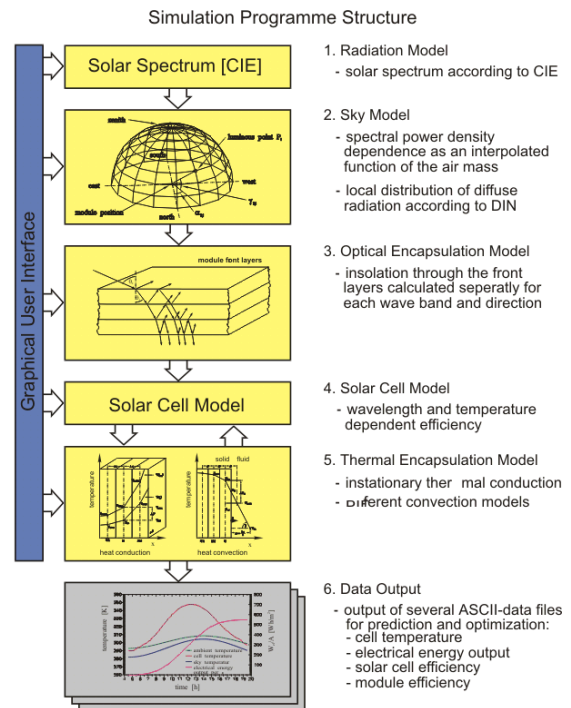


Figure 1: Overview of complete PV module simulation (including thermal part described in [1,4]).

Usually this effect is neglected by the manufacturers due to a lack of treatment measures, but also due to the fact that the electrical interconnections between the cells in the module tend to recompense that effect. Nevertheless, for an accurate modeling and simulation this effect should be taken into consideration. Therefore the simulation program is designed to trace light through all optical interfaces on the way from the real-world environment into the semiconductor material of the cell. This enables the treatment of cells and modules within

the same simulation program.

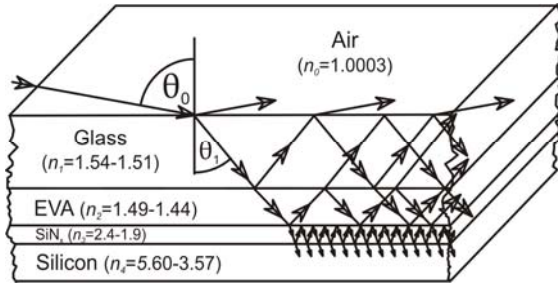


Figure 2: Cross section through a typical PV module together with the traces of a single ray (at the incidence angle θ_0).

1.2 Module to real world interface

Real world also considers actual spectra, irradiance levels and angle of incidence. The angle of incidence for direct solar irradiance throughout a day, together with the elevation angle and the azimuth angle of the sun is illustrated in Figure 3 (plotted for equinox, module elevation angle 36° , latitude 36°)

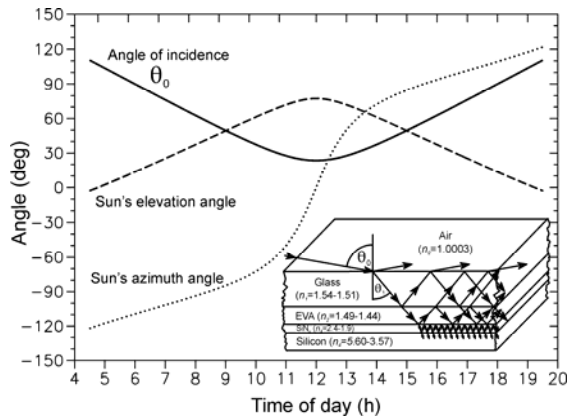


Figure 3: Angle of incidence on a PV module during a day and the path of light through the module encapsulation (right)

2 MODELING OF TRANSMITTANCE

2.1 Single interface

Each optical interface divides an incident ray into a transmitted (T) and into a reflected component (R) according to the Law of Fresnel (see Fig. 4). For perpendicular incidence ($\theta_{in} = 0$) the reflected part is given by:

$$R = \frac{(n_1 - n_0)^2}{(n_0 + n_1)^2} \quad T = 1 - R \quad (1)$$

For non-perpendicular incidence the reflected and transmitted components depend on the state of polarization of the ray towards to the plane of incidence, parallel (\perp) or perpendicular (\parallel):

$$R_{\parallel} = \frac{\tan^2(\theta_{in} - \theta_{out})}{\tan^2(\theta_{in} + \theta_{out})} \quad R_{\perp} = \frac{\sin^2(\theta_{in} - \theta_{out})}{\sin^2(\theta_{in} + \theta_{out})} \quad (2)$$

$$T_{\parallel} = 1 - R_{\parallel} \quad T_{\perp} = 1 - R_{\perp} \quad (3)$$

$$\text{angle of refraction: } \theta_{out} = \arcsin\left(\frac{n_0}{n_1} \sin \theta_{in}\right) \quad (4)$$

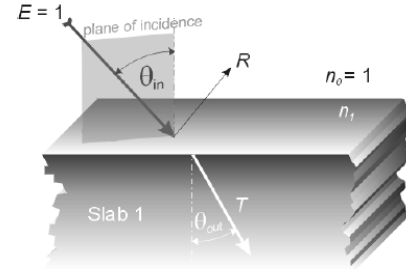


Figure 4: Reflection and transmission at an optical interface.

2.2 Optical slab

Figure 5 shows the situation for an optical slab (or layer) with two optical interfaces and attenuation (or absorption) within the slab.

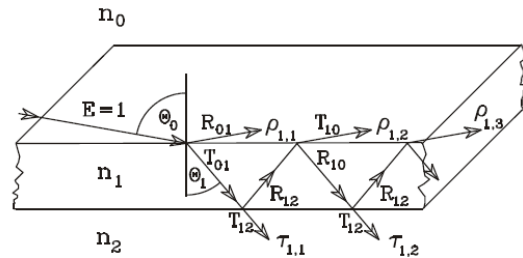


Figure 5: Transmitted and reflected components at an optical slab.

Within the optical slab a ray is bounced at its interfaces infinitely, but with decreasing irradiance levels. If transformed into a so called “geometrical series” the mathematical expression can be simplified. A detailed description of that procedure can be found in [1,2,4].

2.3 Multiple slabs

Considering all possible bounces within the different slabs, among slabs as well as within and among systems of slabs the total transmission equation of a series of slabs is described in [1].

3 TRANSMITTANCE OF ENCAPSULATION

3.4 Results

For the simulation the simulation toolbox as shown in Fig. 1 was used, using the optical part and disabling the thermal part, setting the solar cell temperature to 25°C . As a first result, Figure 6 shows the effect of a variation of the refractive indices of the first two layers on optical transmittance: Optimizing these two layers would result in an increase of 4% in yield. For an incidence angle of 80° , the optimization would even result in an increase of 27% (although at other optimal values of indices of

refraction than for the optimization at perpendicular incidence, as could be seen in Fig. 7).

Figures 9 to 11 show the relevance of the changing spectrum during the day in relation to the spectral efficiency of a solar cell. For single crystalline silicon solar cells the effect of the spectrum's equivalent air mass on the relative electricity yield of the solar cell can reach 5%, as indicated in Fig. 10. The results for other are given in Fig. 11.

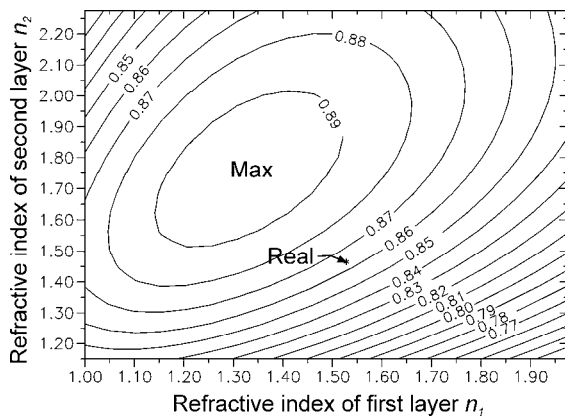


Figure 6: Transmittance of a PV module encapsulation (part of irradiance entering the silicon solar cell at perpendicular incidence) as a function of the refractive indices of the upper two layers. Also indicated is the point of best optical matching (“Max”) and an example of a real PV module (“Real”). The refractive indices of the two lower layers.

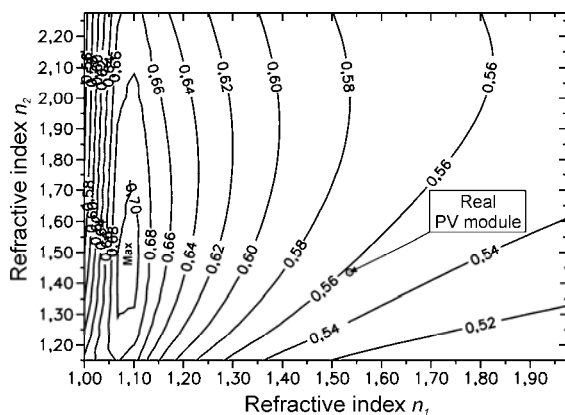


Figure 7: Transmittance of a PV module encapsulation (part of irradiance entering the silicon solar cell at an incidence angle of 80 deg) as a function of the refractive indices of the upper two layers. Also indicated is the point of best optical matching (“Max”) and an example of a real PV module (“Real”).

Figure 8 shows the optical transmission for global irradiance (with modeling of the direct and diffuse components for a clear day) through a module encapsulation during the course of a day at different levels of the model's sophistication. Relative small deviations from the original track of the complete model could be observed if the internal reflections are neglected; this leads to an underestimation of the yield of about 1%. Neglecting optical dispersion results in an overestimation of the yield of about 1.5%. Disregard of lower slabs and the exclusive use of perpendicular

incidence causes vast overestimation of transmittance and therefore should not be applied for modeling.

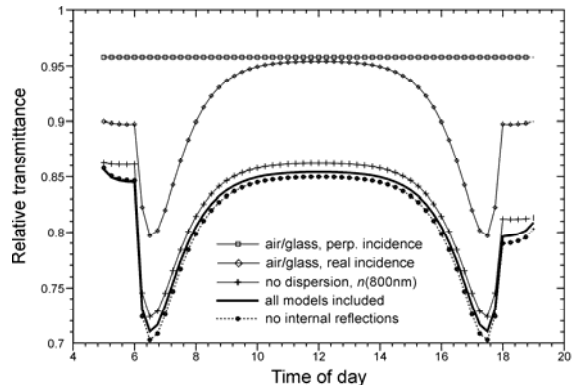


Figure 8: Relative transmittance of module encapsulation during a day for different levels of modeling: From most simple (just first optical boundary with perpendicular incidence) to most detailed (including diffuse irradiance with internal reflections and optical dispersion of encapsulation materials).

A remarkable effect is that the optical performance drops significantly for some time after sunrise (6 a.m.) and before sunset (18 hrs or 6 p.m.). These minima can be explained by high reflection losses of the direct component due to flat incidences. After sunset and before sunrise just the diffuse component is present which suffers from relatively small reflection losses.

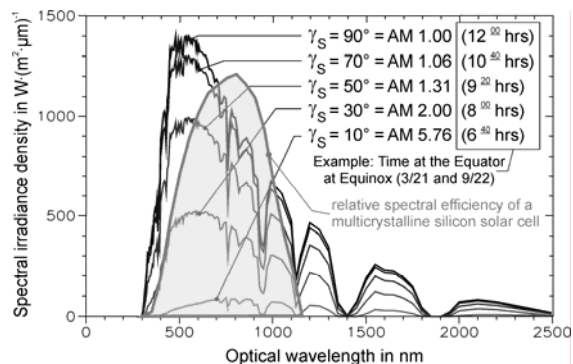


Figure 9: Change of spectra of direct solar irradiance during a clear day, together with the spectral efficiency of a multi-crystalline silicon solar cell.

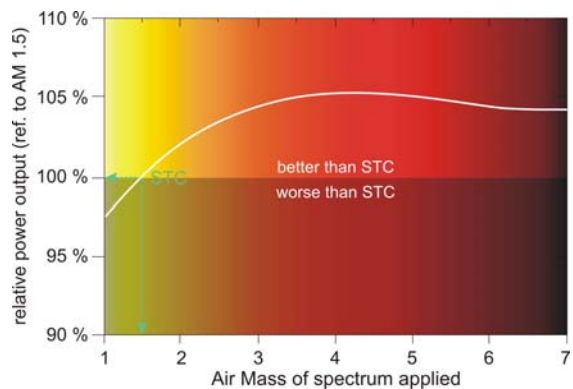


Figure 10: Effect of irradiance spectrum on conversion efficiency and power output of a silicon solar cell.

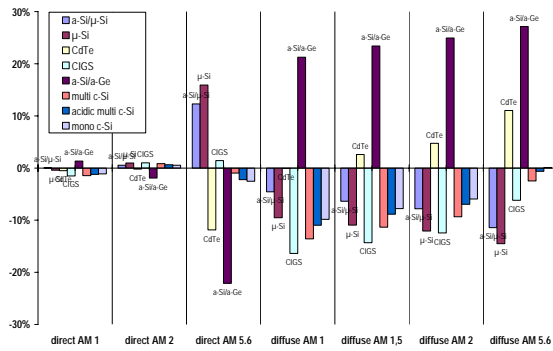


Figure 11: Relative change of power output (via I_{SC}) for several materials and different spectra (rel. to AM 1.5).

Annual electrical energy yield was computed for time intervals of 30 minutes taking into account actual spectra, reflection losses [7], irradiance levels [8] and actual PV conversion efficiency.

Table I: Optical enhancements via an anti-reflective coating on front side of the module cover glass: Gain in annual electrical energy yield at different locations for different refractive indices n_{ARC} of the top anti-reflective layer (module elevation: 30° , composition: ARC, glass, EVA, SiN_x , Si; refractive indices according to [1], SiN_x ($n(600\text{nm})=2.1$).

Location, latitude	n_{ARC}		
	1.21	1.25	1.33
Berlin (lat= 52.5° N)	2.49%	2.41%	1.95%
N-Africa (lat= 30° N)	2.42%	2.36%	1.52%

6 OUTLOOK

Due to actual political conditions most PV power plants are presently not installed in locations where best potentials are, but in the future availability of natural resources in terms of solar irradiance and available land area will become more important most likely. Global solar energy resources are indicated in Fig. 11. It is clearly visible that uppermost potential is available for latitudes in the vicinity of 30° , thus design of solar modules should be adapted accordingly to attend that market with high yield PV systems.

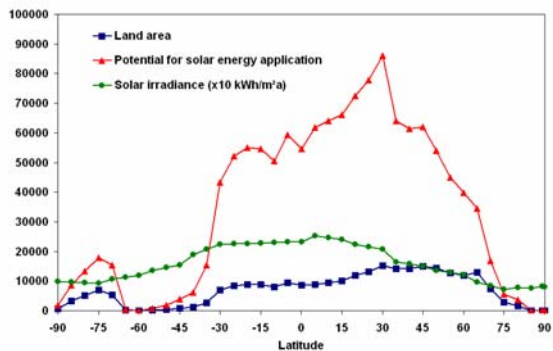


Figure 12: Global solar energy potential given by land mass and solar irradiance as a function of latitude (Krauter/Kissel diagram).

7 CONCLUSION & SUGGESTION

Optical simulation enables considerable improvements for the accurate forecast of annual electrical energy yield of PV generators and allows evaluation of different optical improvements of the module's encapsulation. Performance results provided using standard test conditions are not sufficient to extract the necessary parameters to carry out an accurate yield calculation.

The suggestion is to either provide a complete set of optical, thermal and electrical parameters to fulfill the requirements for an accurate simulation, or to carry out extended tests with different sets of irradiance levels, spectra, and incidence angles to approximate real world conditions. The recommendations given in the working draft of IEC 61853 [6] are a reasonable basis for such extended tests. However, the range of test conditions given should be extended to locations where a large potential for solar electric power generation exists.

8 ACKNOWLEDGMENTS

The authors are very thankful to Philipp Strauß, Kim Onneken, Johannes Kissel, and Norma Blandon for coding of the simulation. Special thanks to Jean François Lelievre from INSA-LPM for providing us his extensive data sets on SiN_x for various NH_3 to SiH_4 ratios.

9 REFERENCES

- [1] Krauter, S: Solar Electric Power Generation, Springer, Heidelberg, New York, 2006.
- [2] S. Krauter, R. Hanitsch, P. Campbell, S. R. Wenham, Proceedings of the 12th European Photovoltaic Solar Energy Conference, Vol. 2 (1994) 1198.
- [3] S. Krauter, R. Hanitsch, Ph. Strauß, Proceedings of "Renewable Energy Sources '91", Prague (CFSR), Vol. 3 (1991) 48.
- [4] S. Krauter, R. Hanitsch, Solar Energy Materials and Solar Cells 41/42 (1996) 557.
- [5] P. Grunow, S. Krauter: Proceedings of 4th World Conference on Photovoltaic Energy Conversion, (2006).
- [6] Performance testing and energy rating of terrestrial photovoltaic (PV) modules IEC 61853 – Working Draft.
- [7] N. Martin, J. M. Ruiz, Solar Energy 22 (2002) 19.
- [8] P. Grunow, S. Lust, D. Sauter, V. Hoffmann, C. Beneking, B. Litzemberger, L. Podlowski, 19th European Photovoltaic Solar Energy Conference (2004).